International Journal of Nanoelectronics and Materials

In Press, Accepted Manuscript – Note to user

Effect of Deposition Direction on the Properties of Silicon layers Fabricated from Recycled Silicon Powder

ALAA A. ABDUL-HAMEAD[1,a]

[1] Materials Engineering Department / University of Technology, Baghdad- Iraq

ABSTRACT

In this research, the recycled silicon R_{Si} nanopowder 50 nm was used to fabricate silicon microwires (SiMWs) arrays by a cold spraying technique (CST). In addition, silicon thin films (SiTFs) of 2μm thickness have been deposited by a thermal evaporation technique (TET). The fabricated SiMWs short length was 0.15-0.6μ0m and the width was 0.1-0.15μm arrays on a glass substrate, after the deposition of the initial silicon sub-layer with a thickness of 50 A˚ as templates by thermal evaporation. Annealing in vacuum at 400 C° was done for both SiMWs and SiTFs. In the CST process, the certified base angles were 0°, 30° and 45°. Diagnostic and optical properties tests of these SiMWs and SiTFs have been done. The results showed that the deposited wires were crystalline with a direction of 111, and by increasing the deposition angle, the transmittance was reduced and the absorbance was increased due to internal reflections among extended SiMWs. The initial annealing of the substrate has assisted in increasing the value of the transmittance when it was compared with the normal thin film, which shows more absorbency, making the fine wire very suitable for solar cells and other optical applications. Consequently, the optical transparency of the SiMWs will be adequate to figure out their alignment.

Key word: Cold spraying, Micro wire, Transmittance, Deposition angle, Internal reflections.

1. INTRODUCTION

Silicon micro wires (SiMWs) arrays have come into concern newly due to the scope they present as highly efficient materials for many applications. A micro-nano technology was able to utilize artificial means for the treatment of materials, which are related within the size category of micro-nano meters. In the 1960s, the arrangement of a large number of microscopic transistors on one chip could establish microelectronic circuits, which enlarge performance, functionality and dependability of electronic devices in a vivid way. This advancement led to the information upheaval, which has made some products like the personal computers, laptops, palmtops and mobile telephones, etc., available [1]. Micro and nano particles are fields which are drawing considerable attention in recent times. The interest in these microscopic particles arises from the advanced properties that appeared due to their small size. These particles find applications in the field of ceramics, catalysis, fuel cells, solar cells, electronics, chemical–mechanical polishing, and data storage [2].

Fabrication of nano wires (NWs) or micro wires (MWs) for silicon or other materials can be produced by many different methods, usually either by bottom-up growth mechanisms or top-down etching processes [3], like chemical vapor deposition (CVD), cold spraying, laser ablation, thermal evaporation, solid reaction, [4], sputter deposition [5], imprint lithography and electro deposition [6]. The researchers noted a difference in most of the properties of

micro-wire compared with thin films for the same materials; this fact has led to think carefully in the fabricated devices and the manufacturing processes [7]. A group of researchers have focused on the preparation conditions effects in SiMWs. Wang et al., [8] used a melt extraction technique to fabricate Fe-6.5wt% Si microwires with 2~30cm in length, with a fan-like microstructure. The authors concluded that the Fe-6.5wt% Si microwires can be successfully used as cores or sensors with high frequency and low induction. Chen et al., [9] fabricated p-type-silicon microwire (p-Si MW) arrays with a length of (10μm) ornamented with amorphous hetero-metal impurity like molybdenum sulfide for water photoelectrolysis via photolithography and dry etching techniques. The p-Si MW was used as a photocathode material for the solar hydrogen evolution. Chen et al., [10] fabricated silicon nanowire 7.8 μm lengthy arrays/WO_3 core/shell photoelectrode, by the metal-catalyzed electroless etching (MCEE) process, after that dip-coating airing and annealing methods were done, for neutral pH water splitting applications. Halima, [11] fabricated a metal-free black silicon which was prepared by metal-assisted wet chemical etching (MaCE), using hydrofluoric acid HF to drive the nano structuring. The heights are 6.4 - 30.8 μm microstructural length depending on the etching time for solar-powered hydrogen generation applications.

Another research focused on optical and electrical properties. J. Hu [12] fabricated hetero-structures made of hierarchical Si core microwires covered by SiO_2 nanowires, which were shaped as multiple junctions to the cores. These structures have been created with a large scale. It can be seen that the Si wires are single crystals with a diameter of about 1–3 μm, while the SiO_2 nanowires are amorphous with a diameter of about 30–80 nm. The materials are expected to become important for optical fibers, low-dimensional waveguides, high-bandwidth optical signal processing devices and scanning near-field optical microscopes. Conventionally, SiMWs were manufactured by many techniques, as mentioned above. In particular, the cold spray technique is affordable. In the cold spray technique (CST), the type and temperature of the gas used are controlled by powder particles in the spraying process [13]. The CST includes the acceleration and impact for a range of solid particles size on a substrate to form a coating with different thicknesses.

The particles are accelerated in a supersonic gas jet which can be produced by the use of a converging–diverging de Laval nozzle. Particles impinging on a substrate will either rebound from the substrate (with or without causing erosion), or bond with the substrate depending on the material type and particle velocity on impact with the substrate. It has been widely reported that many metallic, alloys and composite materials coating can be readily deposited by the cold spray[14,15]. Structural, electrical and optical measurements of SiMWs are the most important properties that are investigated due to their important applications [16]. It is worth mentioning that the Si wires can be used to coat from reduced graphene oxide to enhance photo electro chemical properties [17]. The NWs and MWs arrays have previously been shown to have little reflective losses compared to planar semiconductors. Optical path length and minority carrier diffusion length also should have either a high absorption coefficient or a transcendent light trapping [18]. The good optical properties of SiNWs and SiMWs reduce the cost of solar power by using inexpensive substrates and a lower quantity and quality of the semiconductor material [19]. Silicon nano wires SiNWs, known as nano whiskers, have gained much attention due to their nonpareil physical properties and possible applications in the fields of nano electronics, nano optoelectronics and nano photovoltaics [20].

Wire solar cells fabrications include using even crystalline or amorphous silicon. Other methods of growth techniques include vapor-liquid-solid (VLS) growth, metal-catalyzed chemical etching, molecular beam epitaxial MBE, metal–organic chemical vapor deposition, and deep reactive-ion etching [21]. SiNWs and SiMWs-based solar cells on glass

substrates (which are still finite in the literature) have been fabricated by many methods, due to their promising applications, materials affluence, non poisonous nature, and low cost low-temperature [22]. The knowledge of recycling of the Si wafer to produce a chip or powder preparation is already in use for recycling, and costs associated with recycling are not excessive. V. M. Fthenakis[23] studied the recycling of thin-film solar cells after manufacturing waste. The recycled materials were Tellurium Te, Cadmium Cd and glass. Odo et al., [24] produced nanocrystalline silicon powder in the 100 nm range by using a vibratory disc mill in a top-down synthesis route from single crystalline silicon wafers and a polycrystalline bulk. Cosnita et al., [25] focused on the sustainable recycling of end-of-life silicon photovoltaic (Si-PV) modules. The dismantling of the Si-PV modules (poly-crystalline Si-PV modules) of the Si-PV waste material were prepared by shredding, and then the scraps were milled. Zhao et al., [26] fabricated β-SiC by using recycled waste crystalline silicon, including waste polysilicon (photovoltaic industry), single crystal silicon (waste chip), after crushing and milling. Shin et al.,[27] created an innovative method to the recycle process of recovering silicon (Si) wafer from solar panels. From the above works, it can be seen that an important area of research in this field is the synthesis of micro wires by the cold spraying technique with different deposition angles reflected on sizes, shapes, and controlled disparities of SiMWs structural, electrical and optical properties.

2. EXPERIMENTAL METHODS

2.1 Preparation of Si Powder

The experimental steps to prepare Si powder are listed in Figure (1-a). The waste Si wafer was used and it was crushed to about 1 um, then it was milled by using the ball mill of type (CAPCO English) using a number of mill balls 40 for 3 hours. The particle size test for powder was performed by (Brookhaven Nano Brook 90 plus USA), and the size was less than 50nm, as can be seen in Figure (1-b).

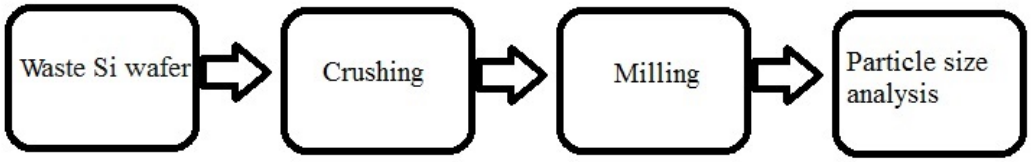

Figure 1(a) The flowchart of Si recycling steps.

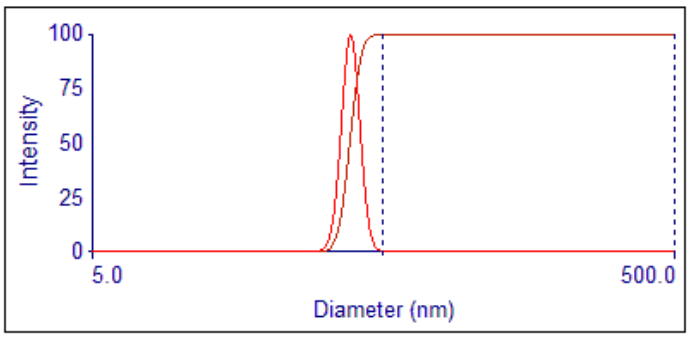

Figure 1(b) The Silicon particle size distribution.

2.1 Preparation of substrates

To fabricate silicon micro-wires SiMWs, growth steps were illustrated as a sketch in Figure 2. The substrates that were used are cleaned laboratory glass slides with dimensions of 2x2x1.2 cm. Preparing sub-films: A thermal vacuumed evaporation technique (TET) of type (EDWARDS) was used to fabricate a film with a thickness of 50A˚ from pure Si powder 99.99%, from US Research Nanomaterials, Inc., which was used. The deposition rate was 2 nm/s at 10^{-4} torr. The distance from the substrate to the evaporation sources was about 12 cm. Annealing was done using a vacuum furnace of type (IVOCLAR), for 30 min at 400C°.

2.2 Preparation of SiMWs and SiTFs

Preparing SiMWs from recycled Si powder by CST: The low-velocity (gas-powder) mixture moves from the feeder into the pre-chamber. Helium gas was used. The spray parameters were; gas temperature 25 Cº at 20 cm distance and 100 Cº substrate temperature, gas to flow was 2.5 ± 0.01 L/min and the pressure was 7bar, as shown in Figure 3. The deposition angle likewise has been changed through changing the basis by angles of 0°, 30° and 45°. Preparing SiTFs from recycled Si powder was also done by a TET, with the same parameters mentioned above. The deposition angle has also been changed through changing the basis by angles of 0°, 30° and 45°, and the thickness was 2μm.

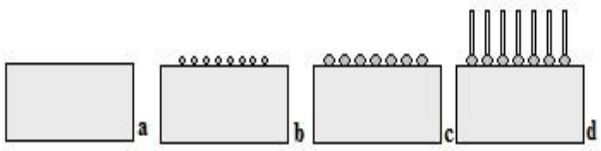

Figure 2: A schematic illustration drawing for the fabrication of SiMWs; a) substrate b) after implantation c) annealing (d) after spraying.

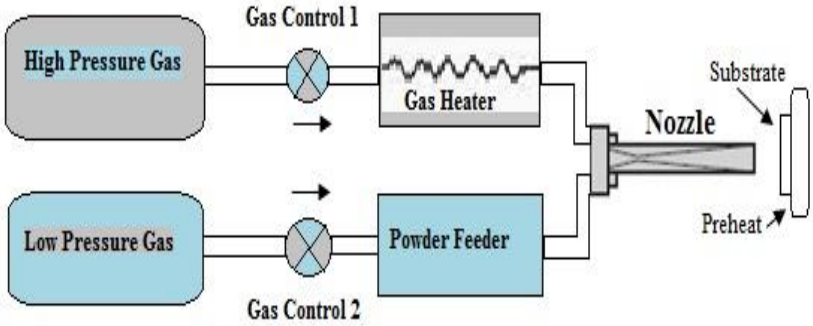

Figure 3: A schematic diagram of the cold spray system.

2.3 Inspection

In order to study the structural properties, the nature and the crystal growth of the deposited films at different deposition conditions, X-ray diffraction XRD measurements have been done by using Philips PW 1050 X-ray diffractometer of (1.5406) Å from Cu-kα. In order to observe the surface topography of deposited thin films, Atomic Force Microscopy (AFM) micrographs were taken with a digital device (AA3000, Angstrom Advanced Inc. USA). The scanning electron microscope SEM (type S-4160) study has been carried out by the Electron

Gun Tungsten heat filament, with a resolution of 3 nm at 30kV and an accelerating voltage of 200V to 30kV, (Japan). The double–beam UV-VIS optical test was done by using (CECIL7200) spectrophotometer from (300-900 nm), to measure the transmittance of the fabricated films and micro-wires. The electrical resistivity was measured directly by an electric prob.

3. RESULTS AND DISCUSSION

3.1 SEM of Sub-layer Results

Figure 4 illustrates the SEM images of the deposited Si sub-layer film surface on the glass substrate after annealing, it can be seen that the growth of close grains of about 0.1 - 0.2 µm to 0.3 - 0.4 µm at the top surface of glass has occurred. The substrate angle of 0˚ in (a) was adopted as the foundation intended for SiMWs and SiTFs growth later; this was stressed by Pan et al. [28].

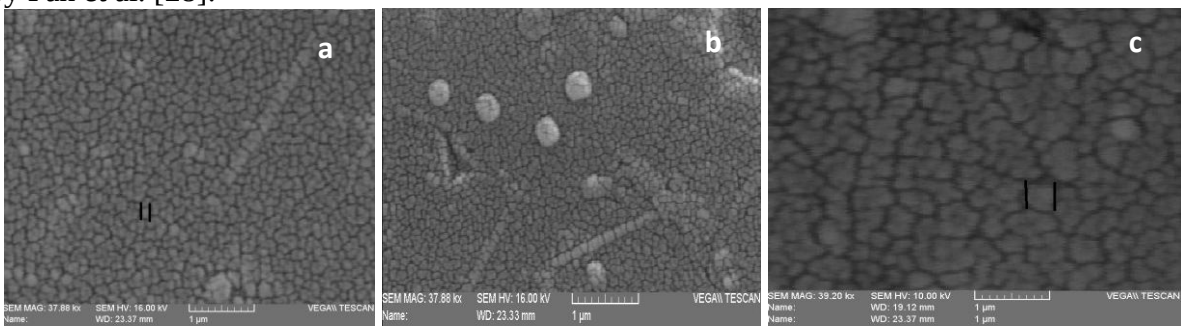

Figure 4:. SEM of Si sub-layer after annealing with different substrate angles; a = 0˚, b = 30˚ and c = 45˚

3.2 X-Ray Diffraction Analysis

Figure 5 shows the XRD results of SiMWs and SiTFs, particularly Figure **(**5 - a, b and c) is for SiMWs and Figure (5 - d, e and f) is for SiTFs. It was found that SiMWs and SiTFs were crystalline, and that SiMWs show higher intensity peak. The diffractograms were recorded in the 2θ range where the most intense reflexes of Si peck are 39.893° and 46.384°, the most prominent peak was found at 39.89° due to the preferred orientation [29, 9], corresponding to Si (111) emphasis cube crystallized, according to Joint Committee on Powder Diffraction Standards JCPDS 35-1158. No peaks appear for any other component, consequently a metal of Si 100% was deposited.

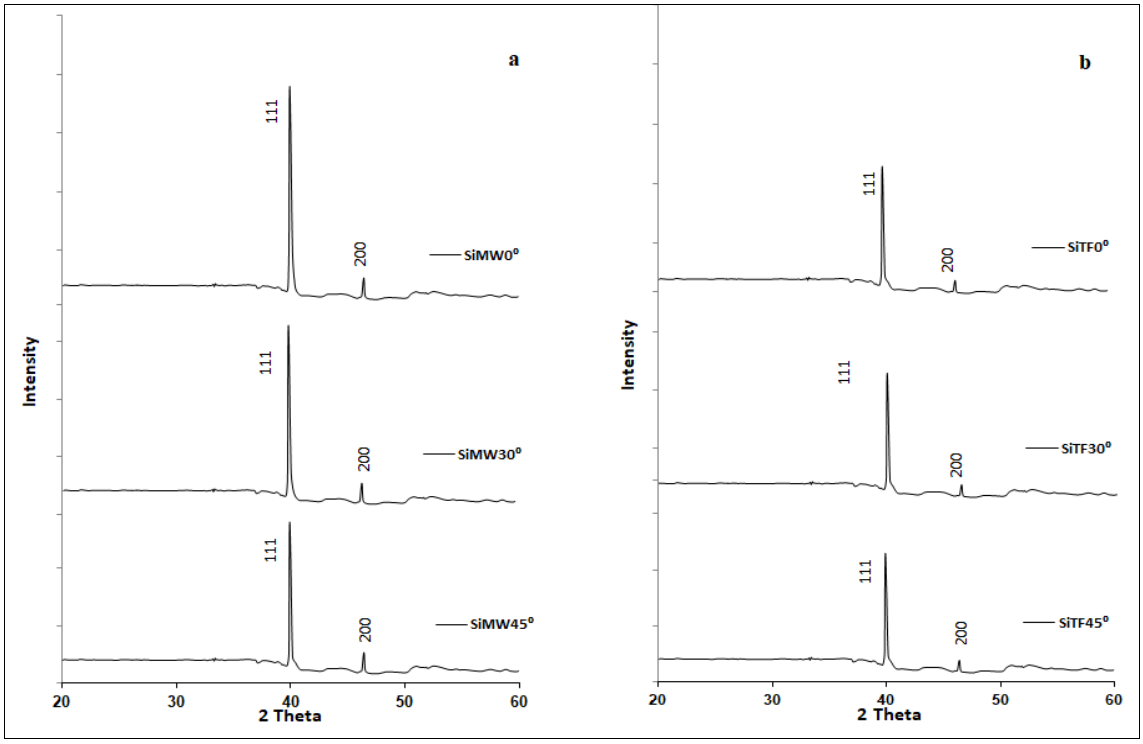

Figure 5: XRD spectrum of films at different substrate angles; a: SiMWs and b: SiTFs.

The scope of investigation of XRD to SiMWs and SiTFs has not been widely considered in the literature, probably E. Gonzalez et al. [29] is the only work. To determine the (a-lattice constant) from the X-ray spectrum, the following formula was used [6, 22]:

$$\frac{1}{d^2} = \left(\frac{h^2 + k^2 + l^2}{a^2} \right) \tag{1}$$

Where d: is the Lattice Plane Spacings (distance between adjacent planes); hkl: are Miller-indices, and a: Lattice Parameter (standard lattice parameter for Si a_{ST} = 3.903). Table 1 shows the structural result of SiMWs and Si SiTFs. Lattice parameter for the SiMWs and the SiTFs were slightly changed with deposition angle.The preferred plane (hkl) in polycrystalline coat, in which there is maximal growth (preferred orientation), can be described by the texture coefficient:

$$T_{c(hkl)} = \left(\frac{I_{m(hkl)} / I_{ASTM(hkl)}}{(\frac{1}{M}) \sum \frac{I_{m(hkl)}}{I_{ASTM(hkl)}}} \right) \tag{2}$$

Where $T_{C\ (hkl)}$ is the texture coefficient of the (hkl) plane, $I_{m(hkl)}$ is the measured intensity, $I_{ASTM(hkl)}$ is the American Standard for Testing Materials ASTM standard intensity of the corresponding powder and M is the number of reflections observed in the X-ray diffraction trace. As shows in Table 1, $T_{C\ (hkl)}$ changes with SiMWs only.

The average crystallite size (C_S) of the SiMWs and the SiTFs were estimated using the Scherrer's formula [13], and it shows in Table 1. Crystallite size increased as deposition angle increased, due to the augmentation in the deposition rate.

$$C_S = \left(\frac{0.94\lambda}{\Delta_{(2\theta)} \cos\theta} \right) \quad (3)$$

Where; λ: is the x-ray wavelength (Å).
$\Delta_{2\theta}$: FWHM; is the Full Width at Half Maximum (radian).
θ: is the Bragg diffraction angle of the XRD peak (degree).

Table 1 Structural result of SiMWs and Si SiTFs.

	SiMWs0°	**SiMWs30°**	**SiMWs45°**	**SiTFs0°**	**SiTFs30°**	**SiTFs45°**
a (nm)	3.900	3.901	3.901	3.902	3.902	3.904
$T_{C\,(hkl)}$	0.951	0.801	0.800	0.902	0.800	0.801
C_S (nm)	67	81	109	89	90	91

3.3 SEM of Films Results

Figure 6 shows the SEM images of SiMWs and SiTFs top view upper surface, representing the effect of deposition angles on the growth direction of the SiMWs in (a, b and c) and SiTFs in (d, e and f). The growth direction is the direction where the most developing Si wires prefer, so affecting the direction for these wires and subsequently affecting the applications. Moreover, in Figure (6-a), it was found that compact wires are aligned in 1-D perpendicular to the direction of the base and it is the perfect state, while (b) and (c) represent angles of 30˚ and 45˚ respectively. In (b), the wires have more thickness and are shorter compared with (a). Where there is a semi-regular shape in Figure (6 - c) and random and tangled shape of wires in Figure (6 -d). Hence, changing the deposition angle affects the way of the growth of the wires on the base, where they have more kinetic energy instead of thermal energy for deposition, enabling them to arrange their growth towards the vertical axis with vertical-alignment and plastic deformation which takes place [30].

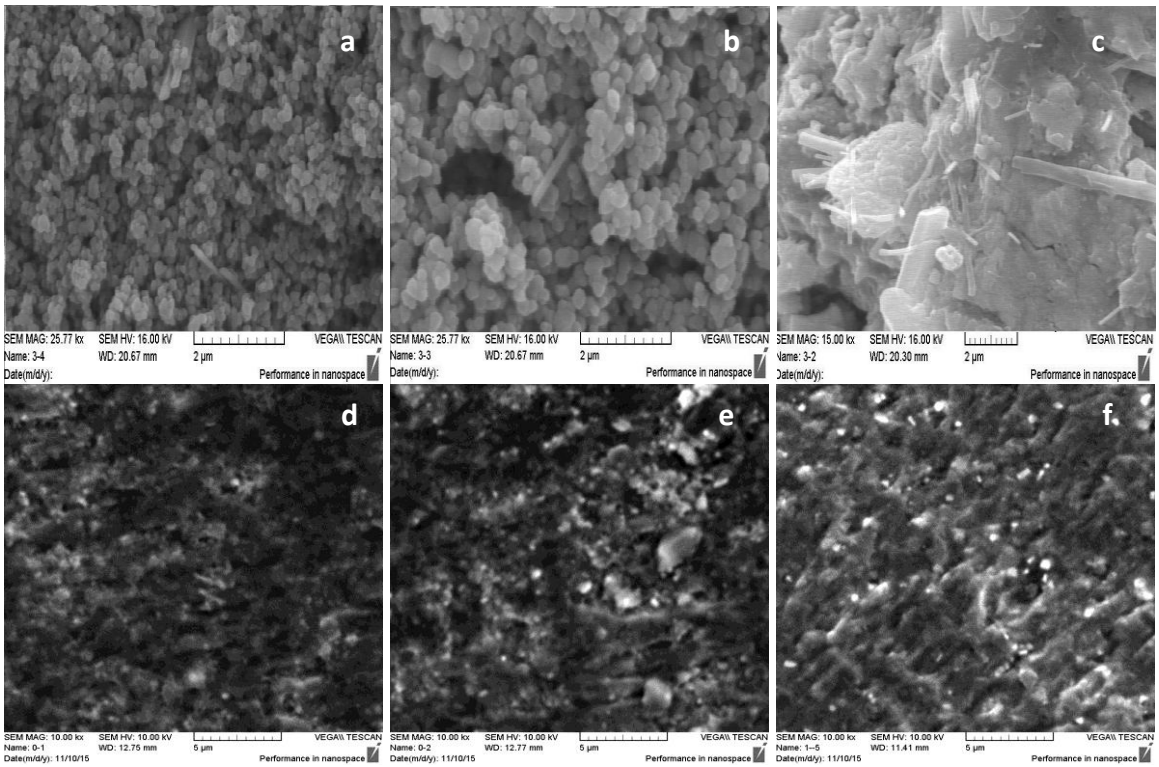

Figure 6: (SEM) top view micrograph image for SiMWs and SiTFs grown on different substrate angles; (a, d) =0˚, (b, e) =30˚ and (c, f) =45˚.

In Figure 7, a represents the surface of the rod-like shaped of Si assembly deposited wires, and precipitated 0˚ angle for substrate with 0.1 µm cross section and more than 1.54 µm length. While in Figure (7 -b), it is 30˚ angle for substrate with 0.15 µm cross section and about 0.6 µm length.

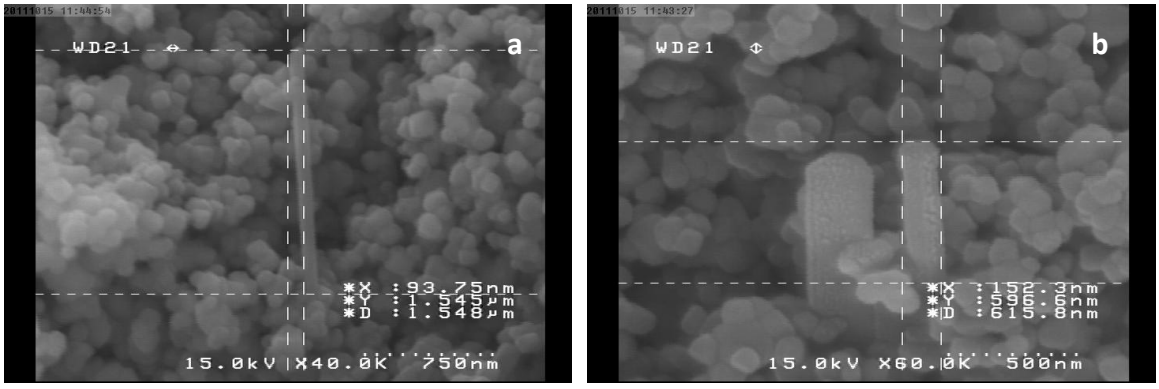

Figure 7: (SEM) A micrograph image for SiMWs at different substrate angles; a = 0 and b = 30˚

3.4 Atomic Force Microscopy Analysis

The AFM results are shows in Figure 8. In particular Figure (8 - a, b and c) are for SiMWs at substrate angles of; a = 0˚, b = 30˚ and c = 45˚, respectively, while Figure (8 - d, e and f) are for SiTFs at substrate angles of; a = 0˚, b = 30˚ and c = 45˚, respectively. SiTFs have almost perfectly smooth

layer surface of the samples which are deposited, while SiMWs have more roughness, because of the influence of the vertical-alignment of SiMWs compared with SiTFs at the same thickness [32]. Table 2 shows roughness parameters of SiMWs and SiTFs.

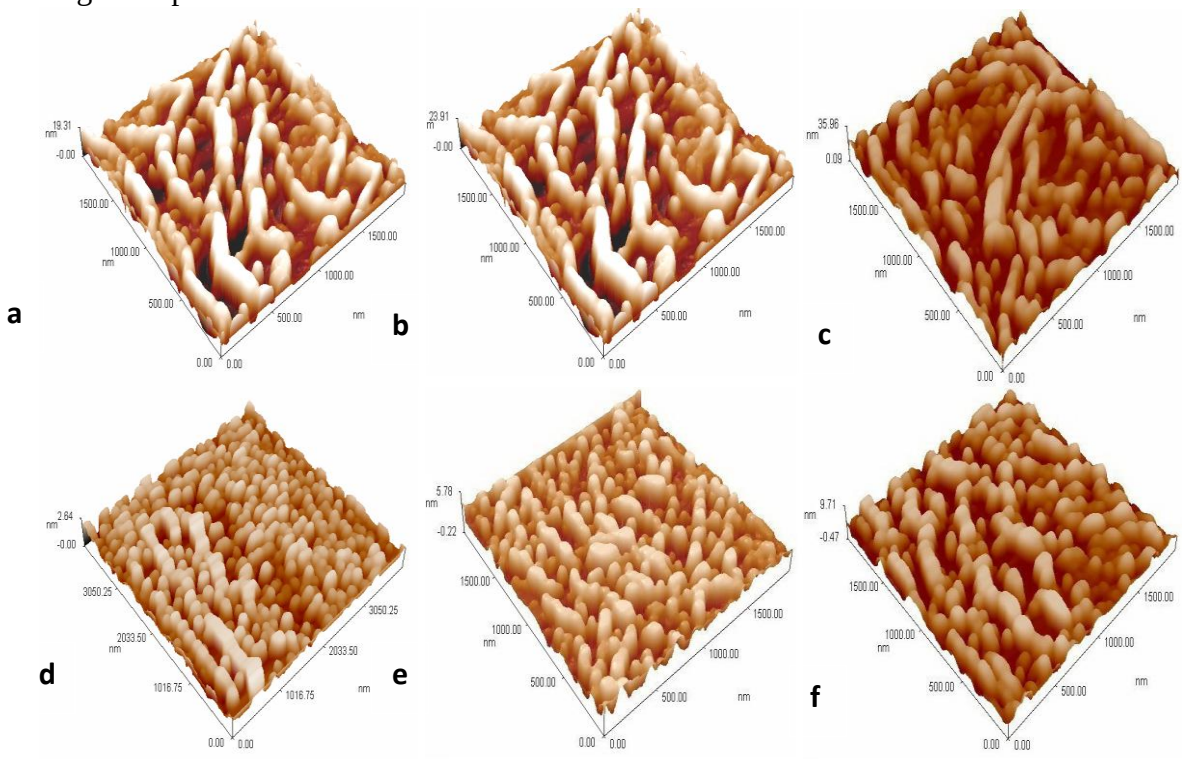

Figure 8: 3D AFM results for SiMWs for different angles; a, b, c and SiTFs in d, e, f.

Table 2 Roughness parameters of SiMWs and SiTFs.

Parameter (nm)	SiMWs0°	SiMWs30°	SiMWs45°	SiTFs0°	SiTFs30°	SiTFs45°
Roughness	19.31	23.91	35.96	2.64	5.78	9.71
Average Diameter	99.77	106.11	122.81	74.83	88.92	93.71

3.5 Optical Transparency

Figure 9 shows the optical transmission spectra results of SiMWs with about 2 μm length and the SiTFs with 2 μm thickness. Figure 9 shows a high transmittance of the SiMWs compared with the SiTFs. Improved transmittance eventuates for SiMWs, making them an anti-reflective system since transmission T is high, the total optical absorption A and reflection R will be low according to R + T + A = 1[31]. SiMWs exhibited an average transmission of ~90% for the entire spectral range of 300-900 nm, whilst SiTFs have an average transmission of ~70% only due to their continues structure form [33] and metal nanostructures formed on a back reflector, which can couple the incident light into the surface plasmon polariton (SPP) modes in which electromagnetic excitations coupled to electron oscillations propagate along the metal-dielectric interface, resulting in sub-wavelength optical confinement.

With increasing the deposition angle of the substrate, the length of the wire was reduced as shown in SEM and the surface roughness results were increased. This increment will reduce the penetration and increase the reflection. Therefore, they have a crucial role in increasing the amount of irradiation transmittance. Also, the particle sizes of the films and wires have a clear effect, as shown in Table 1. The increase in granular size has a negative effect since it is the SiMWs for 67 nm to 109nm elevation about 60%, and a slight difference in SiTFs for 89nm to 91nm only.

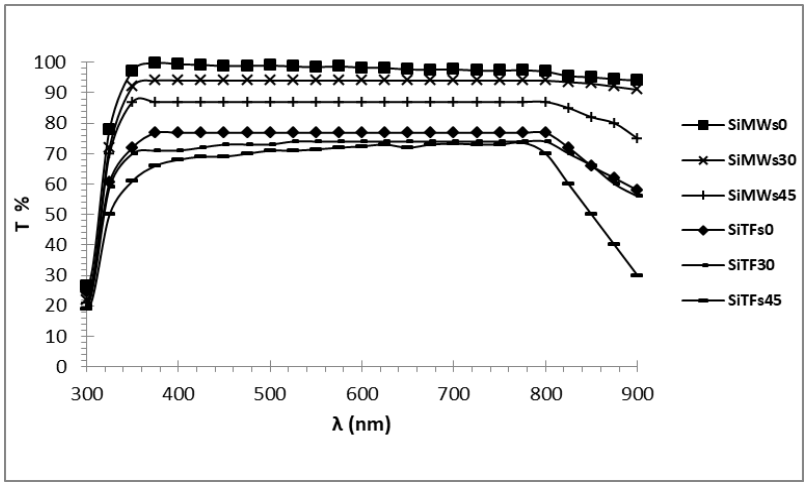

Figure 9: UV-VIS transmission spectra of SiMWs and SiTFs.

Figure 10 shows a diagram of the interaction mechanism of the incident light on the SiMWs and the transmitted light with micro wire alignment, the intensity cross decreases with the increase in the angle of deposition, which means that there is a low access of light beam. It can be realized that uniform SiMWs with low surface roughness force light to pass as shown in Figure 10, micro losses arise from small-scale alignment distortion of SiMWs. The effect of particle sizes of the silicon in the results of XRD, SEM and the AFM for assembled silicon shows a direct proportion to the increase in size and increase in roughness and pre-annealing, which propagates uniformity structure, as shown in Figure **(**5, 6 and 8).

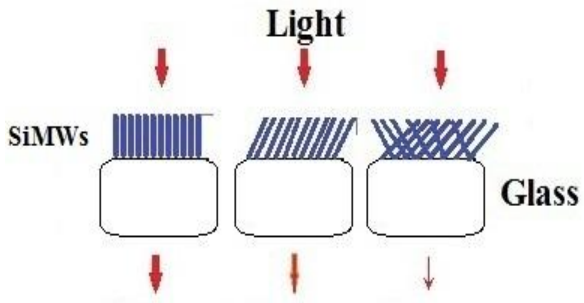

Figure 10: A diagram which shows the light spectra falling on SiMWs deposited at different angles.

3.6 Electrical Resistivity

Anisotropy of the resistivity increases with the directions of the SiMWs. Figure 10 plots SiMWs and SiTFs resistivities at 298 K^{o} as a function of directions of substrate during deposition. The

resistivity of SiMWs is in the range of 350 to 250 Ω-cm, and it decreases as the angle of the substrate increases, which may be due to the increasing cross linking and electric contact points among the array wires when increasing the deposition angle of the substrate, as it can be noted in Figure (7-c). Moreover, SiMWs have a parallel connection between wires and the charge transfer impedance at the electrolyte–semiconductor interface [10].

While the resistivity of SiTFs is in the range of 216 to 240Ω-cm, and it slightly increases as the angle of the substrate increases. This is my be related to the non-homogeneity that takes place in SiTFs at a higher angle, where irregularity is increased as seen in the SEM image in Figure (7- d, e and f). A clear anisotropy is seen for micro-wire widths below 100 nm, with the smallest effect in the (111) direction. The anisotropy of the resistivity becomes less pronounced with increasing the substrate angle until it eventually disappears as the SiMWs resistivity approaches the film resistivity. This increase in resistivity referred to the loss which may have originated from the scattering effect of the electrical conductivity caused by discontinuities in the geometry.

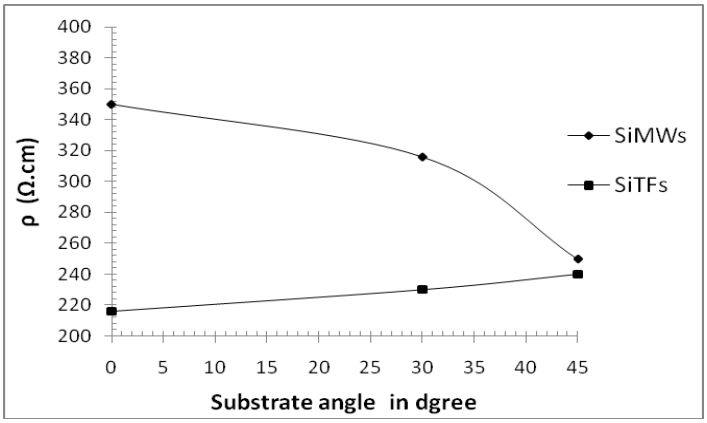

Figure 11: The electrical resistivity of SiMWs and SiTFs with the substrate angle.

4. CONCLUSIONS

The process of recycling the waste silicon wafer from end-of-life with grinding and milling to production of nano particle can be used as a product powder itself, or in the preparation of films or other devices by suitable techniques that can be achieved. The simple cold spraying technique is a reliable method to fabricate SiMWs from recycled Si nanopowder, after choosing the suitable deposition direction and the thermal evaporation technique, which is able to grow Si thin films. The SiMWs were of 0.1-0.15 μm diameter and 0.6-1.54 μm length. Long SiMWs can provide more compatible material structure and fabrication procedures in applications to fabricate optoelectronic devices. Low transmittance means that the alignment of micro silicon wires is decreased and therefore it is not appropriate as a visual window, only at the absorption. This knowledge may help to improve the SiMWs that were utilized as an anti-reflection layer caddying by Si sub-layer is realized with vertical-alignment and high transparency.

REFERENCES

[1] G.A. Mansoori and T.F. Soelaiman,"Nanotechnology–An Introduction for the Standards Community", Journal of ASTM International **2(**2005**)**1-21.

[2] J. Mittal, A. Batra, A. Singh and M.M. Sharma," Phytofabrication of nanoparticles through plant as nanofactories", Adv. Nat. Sci.: Nanosci. Nanotechnol. **5**(2014)1-10.

[3] B. Hoffmann, V. Sivakov, S.W. Schmitt, M.Y. Bashouti, M. Latzel, J. Dluhos, J. Jiruse and S. Christiansen, " Wet – Chemically Etched Silicon Nanowire Solar Cells: Fabrication and Advanced Characterization", Nanowires - Recent Advances, London, INTECH, 2012, pp. 211–230.

[4] H. Suzuki, H. Araki, M. Tosa and T. Noda, "Formation of silicon nanowires by CVD using gold catalysts at low temperatures", Mater. Trans.**48**(2007) 2202-2206.

[5] M.R. Shaner, S. Hu, K. Sun and N. S. Lewis, "Stabilization of Si microwire arrays for solar-driven H_2O oxidation to O_2(g) in 1.0 M KOH(aq) using conformal coatings of amorphous TiO_2", Energ. Environ. Sci.**8**(2015)203-207.

[6] H.A. Audesirk, E.L. Warren, J. Ku and N.S. Lewis, "Ordered silicon microwire arrays grown from substrates patterned using imprint lithography and electrodeposition", ACS Appl. Mater. Interfaces.**7**(2015)1396-1400.

[7] A.K. Palai, J. Lee, T.J. Shin, A. Kumar, S.U. Park and S. Pyo, "Solution-grown single-crystalline microwires of a molecular semiconductor with improved charge transport properties", Chem. Commun.**50**(2014)8845-8848.

[8] S. Wang, Y. Liang, F. Ye, G. Geng and J. Lin, "Microstructure, mechanical and magnetic properties of melt extracted Fe-6.5 wt.%Si microwires", J. Mater. Process. Tech. **249**(2017)325-330.

[9] C.J. Chen, K.C. Yang, C.W. Liu, Y.R. Lu, C.L. Dong, D.H. Wei, S.F. Hu and R.S. Liu," Silicon Microwire Arrays Decorated with Amorphous Heterometal-doped Molybdenum Sulfide for Water Photoelectrolysis" Nano Energy **32** (2017)422-432.

[10] Z. Chen, M. Ning, G. Ma, Q. Meng, Y. Zhang, J. Gao, M. Jin, Z. Chen, M. Yuan, X. Wang, J. Liu and G. Zhou, "Effective silicon nanowire arrays/WO_3 core/shell photoelectrode for neutral pH water splitting", Nanotecnology **28**(2017)1-24.

[11] A. F. Halima, X. Zhang and D. R. MacFarlane,"Metal-Free Black Silicon for Solar-powered Hydrogen Generation", Electrochim. Acta. **235** (2017) 453-462.

[12] J. Hu, Y. Bando, J. Zhan, X. Yuan, T. Sekiguchi and D. Golberg,"Self-assembly of SiO_2 nanowires and Si microwires into hierarchical heterostructures on a large scale", Adv. Mater. **17** (2005)971–975.

[13] T. P. Singh, "Investigation of Flow Parameters for Titanium Cold Spraying using CFD Simulation", MsC thesis, The University of Waikato, New Zealand (2010).

[14] S. R. Bakshi, D. Wang , T. Price, D. Zhang, A. K. Keshri, Y. Chen, D. Graham McCartney, P. H. Shipway and A. Agarwal, "Microstructure and wear properties of aluminum/aluminum–silicon composite coatings prepared by cold spraying", Surf. Coat. Tech. **204**(2009)503–510.

[15] W.Y. Li, C. Zhang, X. P. Guo, G. Zhang, H. L. Liao and C. Coddet, "Deposition characteristics of Al–12Si alloy coating fabricated by cold spraying with relatively large powder particles", Appl. Surf. Sci. **253**(2007)7124-7130.

[16] M.D. Kelzenberg, D.B. Turner-Evans, M.C. Putnam ,S.W. Boettcher, R.M. Briggs, J.Y. Baek, N.S. ewis and H.A. Atwater," High-performance Si microwire photovoltaics", Energ. Environ. Sci. **4**(2011) 866-871.

[17] Z. Huang, P. Zhong, C. Wang, X. Zhang and C. Zhang, "Silicon Nanowires/Reduced Graphene Oxide Composites for Enhanced Photoelectrochemical Properties", ACS Appl. Mater. Inter. **5**(2013)1961-1966.

[18] E. Garnett and P. Yang,"Light Trapping in Silicon Nanowire Solar Cells", Nano. Lett. **10**(2010)1082-1087.

[19] C. M. Lieber and Z. L. Wang, "Functional Nanowires", MRS Bull. **32**(2007)99-108.
[20] X. Duan, Y. Huang, R. Agarwal and C.M. Lieber,"Single-nanowire electrically driven lasers", Nature 421(2003) 241-245.
[21] M.C. Putnam, S.W. Boettcher, M.D. Kelzenberg, D.B. Turner-Evans, J.M. Spurgeon, E.L. Warren, R.M. Briggs, N.S. Lewis and H.A. Atwater, "Si microwire-array solar cells", Energ. Environ. Sci. **3**(2010)1037-1041.
[22] V. Sivakov, G.Andra, A. Gawlik, A. Berger, J. Plentz, F. Falk and S.H. Christiansen,"Silicon Nanowire-Based Solar Cells on Glass: Synthesis, Optical Properties, and Cell Parameters", Nano. Lett. **9**(2009)1549-1554.
[23] V.M. Fthenakis, "End-of-life management and recycling of PV modules", Energy Policy **28** (2000)1051-1058.
[24] E.A. Odo, D.T. Britton, G.G. Gonfa and M. Harting,"Mechanism of DC conduction in silicon nanoparticles network", The African Review of Physics **7**(2012) 45-56.
[25] M. Cosnita, C. Cazan, A. Duta, and I. Visa, "Recycling Silicon-PV Modules in Composites with PVC, HDPE and Rubber Wastes", Springer Proceedings in Energy (2017) 375-394.
[26] M. Zhao, M. Johnson, W. He, G. Li, C. Zhao, J. Huang and H. Zhu, "Transformation of waste crystalline silicon into submicro β-SiC by multimode microwave sintering with low carbon emissions", Powder Technol. **322**(2017) 290–295.
[27] J. Shina, J. Parkb and N. Parka, " A method to recycle silicon wafer from end-of-life photovoltaic module and solar panels by using recycled silicon wafers", Sol. Energ. Mat. Sol. C **162**(2017) 1-6.
[28] Z. W. Pan, Z. R. Dai, L. Xu, S. T. Lee, and Z. L. Wang," Temperature-Controlled Growth of Silicon-Based Nanostructures by Thermal Evaporation of SiO Powders", J. Phys. Chem. B 105(2001)2507-2514.
[29] E. Quiroga-Gonzalez, J. Carstensen and H. Foll,"Structural and Electrochemical Investigation during the First Charging Cycles of Silicon Microwire Array Anodes for High Capacity Lithium Ion Batteries", Materials **6**(2013) 626-636.
[30]A. Moridi, S.M. Hassani-Gangaraj, M. Guagliano and M. Dao,"Cold spray coating: review of material systems and future perspectives", Surf. Eng. **30**(2014)369-395.
[31] Y.J. Hung, S.L. Lee, K.C. Wu, Y. Tai and Y.T. Pan, "Antireflective silicon surface with verticalaligned silicon nanowires realized by simple wet chemical etching processes", Opt. Express. **19**(2011)15792-15802.
[32] S. D. Jiang, T. Eggers, O. Thiabgoh, D.W. Xing, W. D. Fei, H.X. Shen, J. S. Liu, J. R. Zhang, W. B. Fang, J. F. Sun, H. Srikanth and M. H. Phan,"Relating surface roughness and magnetic domain structure to giant magneto-impedance of Co-rich melt-extracted microwires", Sci. Rep-UK **7**(2017)1-8.
[33] K.T. Park, Z. Guo, H.D. Um, J.Y. Jung, J. M. Yang, S. K. Lim, Y.S. Kim, and J.H. Lee1," Optical properties of Si microwires combined with nanoneedles for flexible thin film photovoltaics", Opt Express **19**(2011) A41-A50.